field on the two types of planes. Generally for the olivine structure it is necessary to know the concentration of the major elements with reasonable accuracy, but in the present case, where we have already established that 50 percent of the Mg atoms occupy each M site, the analysis becomes particularly simple. The number of x-ray counts from any element Y in a spectrum is given by

$$N_{\mathrm{Y}} = k_{\mathrm{Y}} C_{\mathrm{Y}} I_1 + k_{\mathrm{Y}}(1 - C_{\mathrm{Y}}) I_2 \qquad (2)$$

where I_1 and I_2 are, respectively, the electron intensities on the M1 and M2 planes integrated over time and thickness, C_{Y} is the fraction of element Y on the M1 sites, and k_{Y} is a constant which depends on the efficiency of the spectrometer. From one spectrum taken under such conditions that the electron wave field is modulated ($I_1 \neq I_2$) and one with a uniform wave field ($I_1 = I_2$), the occupancy C_{A} for an element A can be shown to depend only on N_{Si}, N_{Mg}, and N_{A} as obtained from the two spectra. The analysis used to determine C_{Fe}, C_{Mn}, and C_{Ni} in Table 1 is essentially as described above. However, in order to improve the statistical accuracy, three spectra were used for each measurement. For two of the spectra the incident beam directions were as in Fig. 1, and for the third spectrum strong reflections were avoided so that $I_1 = I_2$ [see (*5*) for details]. Despite the variations in *R*(Si/Mg), *R*(Si/Fe), and *R*(Si/Ni), which result from slightly different experimental conditions of thickness and orientation, the site occupancies derived from these *R* values agree closely. From Table 1 we obtain $C_{\mathrm{Fe}} = 49.6 \pm 1$ percent, $C_{\mathrm{Mn}} = 1 \pm 5$ percent, and $C_{\mathrm{Ni}} = 97 \pm 5$ percent.

Except for Fe, these site preferences agree with those predicted by Burns (*6*) for an Mg-olivine. It is, however, well known that theory fails to predict the Fe occupancy, and the surprising result that both Fe and Mg have similar site preferences between dissimilar sites has been confirmed in other experiments, such as that by Burns (*6*) on natural olivine with the use of optical absorption spectroscopy. Studies of synthetic and heat-treated Mg-Mn (*7*) and Mg-Ni (*8*) olivines show a much lower degree of ordering, an indication that the complete ordering of Mn and Ni found in our study is characteristic of a rock that is slowly cooled. The two main factors governing site preference in olivines are thought to be cation size and crystal field stabilization energy. For Fe, these factors are believed to compensate each other completely. It is known that Mn^{2+} experiences no crystal field effect, and the size of Mn^{2+} relative to Mg^{2+} indicates that the Mn atoms should occupy the larger M2 site. Since there is little size difference between Ni and Mg, Ni appears strongly influenced by crystal field effects. However, the prediction of cation site preferences is far from simple, and a large number of factors may influence the result (*9*).

Our results demonstrate that the orientation dependence of electron-induced characteristic x-ray emission can be used to determine quite accurately the cation distribution in olivine and also that of the trace elements. To our knowledge, no other single technique is capable of doing this for the small areas, low concentrations, and neighboring elements used in this study. Few assumptions have been made, the main one being that the localization of the various K_{α} processes is the same. A small systematic error may thus be introduced. However, the results of other workers (*10*) suggest that this effect is unlikely to affect C_{X} by more than 1 percent. For more complicated structures, dynamical calculations can be used in conjunction with quantitative analysis. It is expected that the method will be useful for the elucidation of many crystal structures in addition to the spinel, olivine, and sphalerite structures already studied (*5, 11*).

J. TAFTØ
J. C. H. SPENCE

Department of Physics,
Arizona State University,
Tempe 85287

References and Notes

1. H. R. Wenk, Ed., *Electron Microscopy in Mineralogy* (Springer-Verlag, New York, 1976).
2. J. W. Knowles, *Acta Crystallogr.* **9**, 61 (1956).
3. B. W. Batterman, *Phys. Rev. Sect. A* **133**, 759 (1964).
4. D. Cherns, A. Howie, M. H. Jacobs, *Z. Naturforsch Teil A* **28**, 565 (1973).
5. J. Taftø, *J. Appl. Crystallogr.*, **15**, 378 (1982).
6. R. G. Burns, *Am. Mineral.* **55**, 1608 (1970).
7. C. A. Francis and P. H. Ribbe, *ibid.* **65**, 1263 (1980).
8. V. Rajamani, G. E. Brown, C. T. Prewitt, *ibid.* **60**, 292 (1975).
9. D. L. Bish, *ibid.* **66**, 770 (1981).
10. A. J. Bourdillion, P. G. Self, W. M. Stobbs, *Philos. Mag. A* **44**, 1335 (1981).
11. J. Taftø and Z. Liliental, *J. Appl. Crystallogr.* **15**, 260 (1982); J. Taftø and J. C. H. Spence, *Ultramicroscopy*, in press.
12. We acknowledge the support provided by the staff of the NSF High-Resolution Electron Microscopy facility at Arizona State University and useful discussions with J. Smyth, M. O'Keeffe, and P. Buseck for the provision of specimens. This research was funded under NSF grant DMR8002108.

29 April 1982; revised 6 July 1982

Hydration Aging of Nuclear Waste Glass

Abstract. *The aging of simulated nuclear waste glass by contact with a controlled-temperature, humid atmosphere results in the formation of a double hydration layer penetrating into the glass and in the formation of minerals on the glass surface. The hydration process described here provides insight into the aging kinetics of naturally occurring glasses and also suggests that simulated aging reactions are necessary for demonstrating that nuclear waste forms can meet projected Nuclear Regulatory Commission requirements.*

Two facets of glass hydration are of current interest. The extent of surface hydration offers archeologists a method of dating prehistoric (*1, 2*) and more recent man-made (*3*) artifacts. The reverse process, the aging of simulated glass through induced hydration, can help to provide a sound, demonstrable technical basis for predicting the long-term performance of nuclear waste glass (*4*).

The hydrated layer (perlite) that forms on natural glasses has a higher water content (~ 3.5 percent by weight) than the bulk glass (~ 0.1 percent). This layer has been observed microscopically under polarized light and with either $^{15}\mathrm{N}$ (*5*) or $^{19}\mathrm{F}$ (*6*) nuclear resonance depth profiling. The hydrated layer forms by the exchange of mobile alkali metal ions from the bulk glass with protons, during which process the silicate network is believed to remain virtually unchanged (*7*). Tsong *et al.* have shown (*8*) that, in obsidian, surface hydration is accompanied by dealkalization and a buildup of calcium and magnesium in the outermost layers. The reaction kinetics ascribed to both field samples and simulated laboratory glasses were initially shown to follow a $t^{1/2}$ diffusion-type rate equation, where t is time (*1, 2*). However, other experimenters, using field samples, have had difficulty reproducing this rate law and report a time dependence ranging from $t^{1/3}$ to t^3 (*9*).

These disparate results have been attributed to an incomplete knowledge of weathering conditions and to less-than-rigorous segregation of glasses having different compositions. Clearly, composition, temperature, and water vapor concentration affect layer formation. It is possible that the differences between natural and simulated hydration cannot be reconciled (*10*), but certainly the dating of natural specimens on the basis of hydration is valid only if the glass compositions and past climatic conditions are specified and if the hydration kinetics of the glass are established (*9*).

Glass hydration is also of interest to those engaged in the management of nuclear waste. The transport of radioactive nuclides from waste packages in a repository to the biosphere is most likely to occur as a result of direct contact with ground water. Proposed Nuclear Regulatory Commission regulations (*11*) contemplate a period of waste confinement of at least a thousand years during which no transport would occur. Nevertheless, most release studies to date have focused on freshly cut waste forms (*12*). However, contact of waste with ground water, if it occurs, will probably take place after the waste has aged in the repository environment. Thus, studies with unaged waste might not be addressing the issues germane to reducing the technical uncertainties of waste disposal.

Some aging effects (for example, devitrification and irradiation damage) have been studied individually (*12*), but, as far as we are aware, no detailed studies have been reported on aging as a result of hydration. Hydration will be a primary mode of aging waste glass in an unsaturated zone, given conditions of elevated temperatures, available ground water, and a breached containment.

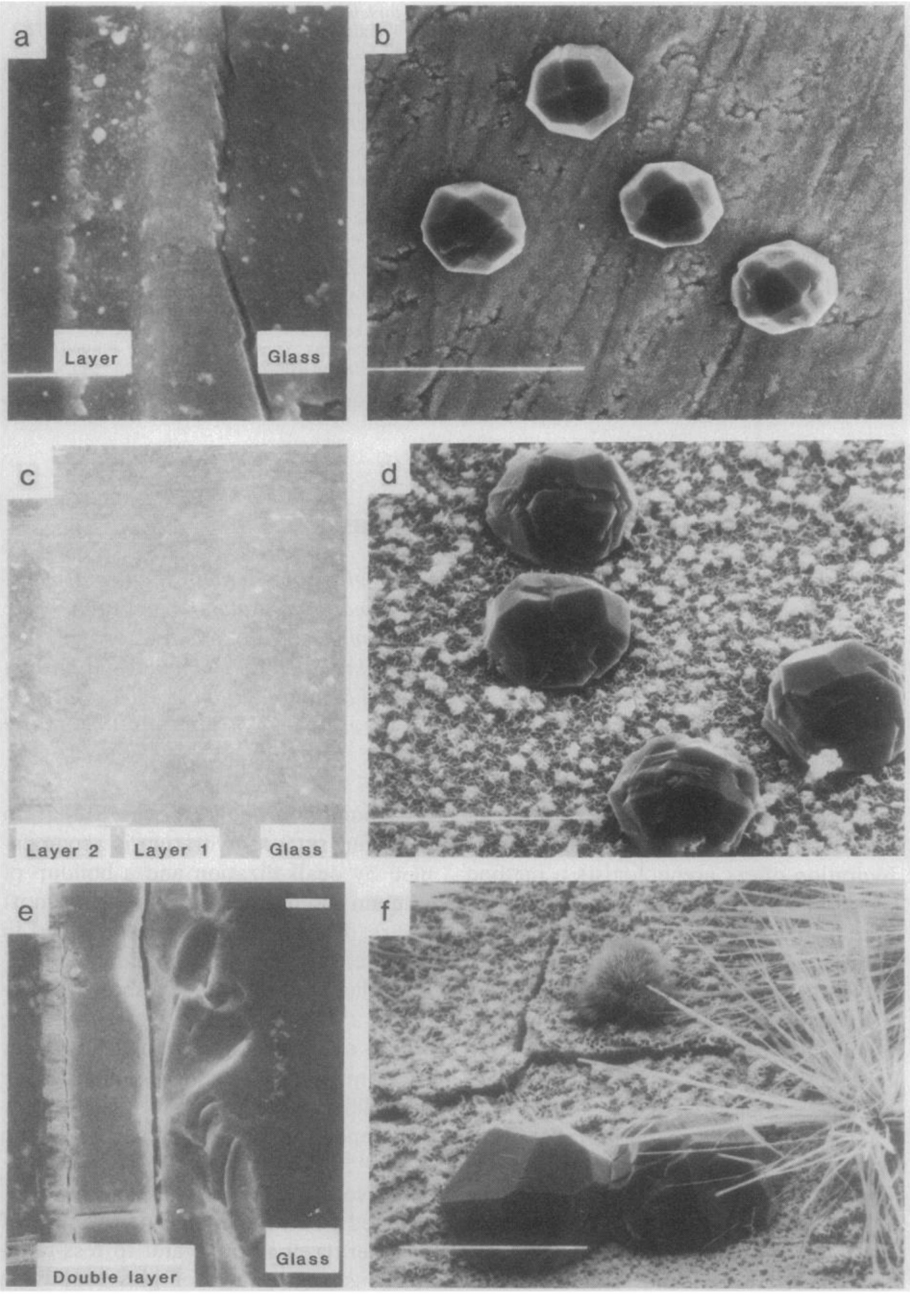

Fig. 1. A series of SEM photomicrographs of hydrated (202°C) SRL 131 glass: (a) cross section showing a single hydrated layer, 6 hours exposure, scale = 5 μm; (b) surface showing analcime formation, 6 hours, scale = 50 μm; (c) cross section showing a double-layer formation, 24 hours, scale = 5 μm; (d) surface showing analcime formation and surface alteration, 24 hours, scale = 50 μm; (e) cross section showing advanced double-layer formation, 192 hours, scale = 8.5 μm; and (f) surface showing analcime and tobermorite formation, 192 hours, scale = 95 μm.

Work reported here on the hydration of typical nuclear waste glasses under controlled conditions suggests that alterations due to aging may have significant effects on the leaching of glass. These results may also impact on the reported divergence in the time dependence of the hydration layer thickness observed for natural glasses.

Two borosilicate glasses, 211 and 131, developed by Savannah River Laboratory (SRL) for the encapsulation of nuclear defense waste, were used in this study (*12*). The major components of glasses 131 and 211 (in percentage by weight by oxide) are as follows: Si, 45 and 44; Na, 13 and 15; Fe, 14 and 11; B, 11 and 8; Ca, 1 and 5; Mn, 3 and 3; Al, 3 and 3; Li, 4 and 3; and Ni, 2 and 2. The homogeneity of the glass has been established on the basis of an energy-dispersive x-ray analysis (EDAX) for the matrix elements and neutron activation analysis for the waste elements.

Hydration tests were done at 120°, 202°, and 240°C. These tests differ from hydrothermal leach tests in that only enough water was used to yield saturated water vapor conditions when at temperature, and at no time was the glass contacted by liquid water. The glass samples were suspended by a Teflon thread and held in the center of a tantalum-lined reaction vessel. We terminated the tests by quenching the vessel in water to avoid the formation of condensate on the samples. One-half of each sample was mounted and polished, and the cross section was studied by scanning electron microscopy (SEM) and EDAX. The surface of the other half was studied by x-ray diffraction (XRD) in addition to SEM and EDAX. A detailed description of the procedures used in these experiments is given in (*13*).

A sequence of cross-section and surface photomicrographs is shown for hydrated SRL 131 glass in Fig. 1. In this series, with hydration at 202°C for 6 hours to 14 days, several different crystalline species were observed to form on the glass surface, until after 14 days the surface was completely covered with a white, fibrous layer. The trapezohedral crystals, evident after only 6 hours, are analcime, a mineral belonging to the zeolite family and having the composition $NaAlSi_2O_6 \cdot H_2O$. The individual crystals grow to a size of 100 μm. The fibrous mineral, evident only after 8 days of hydration but completely covering the surface after 14 days, is tobermorite, $Ca_5(OH)_2Si_6O_{16} \cdot 4H_2O$, one of the main constituents of concrete. The glass surface itself also appears to be altered (Fig. 1, c and d) and is transformed into a secondary crystalline layer up to 5 μm thick. This mineral layer has not been identified unambiguously but belongs to the montmorillonite group of clay minerals. The XRD results indicate that this layer is similar to stevensite, $(Mg_{2.88}, Mn_{0.02}, Fe_{0.02})Si_4O_{10}(OH)_2 \cdot (Ca,Mg)_{0.07}$.

The structure of montmorillonite-type minerals is always unbalanced because of atomic substitutions in their expandable layer structure. The resulting deficiency of net positive charge is balanced by exchangeable cations adsorbed between the unit layers and around their edges. As with minerals of the montmorillonite group, analcime is able to incorporate waste elements into its structure. The cesium analog to analcime is pollucite, and a continuous series of sodium-cesium compositions is possible during mineral formation. Once incorporated, the cesium is locked in the mineral and is nonexchangeable.

Similar minerals form on the surface of SRL 211 glass, but the advent of tobermorite formation and complete coverage of the glass surface occurs much faster than for SRL 131 glass. A calcium elemental profile (EDAX) of the SRL 211 layer cross section that had been hydrated for only 6 hours indicates a rapid buildup of calcium near the glass surface.

The cross sections of the reacted glasses show that the hydrated layer consists of two parts: a thicker (inner) layer that is nearly depleted of sodium and partially depleted of aluminum and calcium and a thinner (outer) montmorillonite-type layer as discussed above. The thicker layer appears to be very similar to the bulk glass, but the interface between the layer and the glass, as marked by the sodium profile, is very sharp. When a thick hydration layer is formed on the glass surface, cracking occurs, possibly during humid conditions but certainly on quenching and drying. Such cracks may not exactly reproduce those formed during waste storage but would provide additional channels through which liquid water could contact the glass, whereupon leaching could occur or be accelerated.

The thickness of the hydrated layer was taken to be the total depth from the "surface" of the glass to the maximum extent of sodium depletion (Fig. 1) and includes both layers. This thickness is plotted as a function of time in Fig. 2 for both SRL 131 and SRL 211 glasses hydrated at 202°C. Each curve has two distinct regions, an initial segment that is linear with $t^{1/2}$ and a second region with a steeper slope for which there are not enough data to establish the functionality in t. The change in hydration rate might be related to the cracking that occurs as the layer becomes thicker or might be due to a change in the mechanism that occurs with the appearance of tobermorite on the surface. Data at this time are insufficient to establish a detailed explanation. Similar curves have been obtained for glass hydrated at 240°C, and these show the onset of the steeper portion of the curve occurring sooner than for glass hydrated at 202°C. At 120°C or below, observation of the second part of the hydration process would require extended exposure.

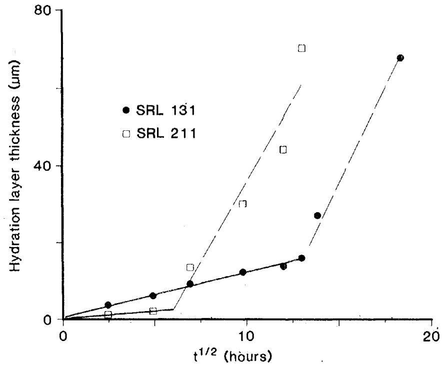

Fig. 2. The time-temperature relationship of two nuclear defense glasses hydrated at 202°C. The dashed lines indicate that the reaction rate has increased but that the functional relationship between time and temperature is not known.

From the values of the hydration rate, k, determined at 120°, 202°, and 240°C for the first portion of the time-temperature curves, it is possible to fit the data to the Arrhenius equation,

$$k = Ae^{-E/RT}$$

where A is a constant, E is the activation energy of reaction, R is the gas constant, and T is the temperature. Although the data are limited, the relation of ln k and $1/T$ is linear and for SRL 131 glass yields an E of 17,900 cal/mole and an A of 1.9×10^{15} μm^2 per 1000 years. This suggests that the mechanism of the initial hydration reaction does not change between 120° and 240°C. This conclusion is reinforced by the observation of the same surface features for glass hydrated at each temperature.

Although there are differences in composition between natural rhyolitic glass and nuclear waste glass that may influence the hydration mechanism, the E values for waste glass derived from the first portion of the curves are very similar to those calculated for obsidian (*2*), that is, E ranging from 19,200 to 21,600 cal/mole with A ranging from 1.4×10^{15} to 18×10^{15} μm^2 per 1000 years, and with $t^{1/2}$ kinetics the same as those determined in layer thickness by Friedman and Long (*2*). However, if we replot the present results using the error limits pertinent to earlier data (*9*), a single rate, linear in $t^{3/2}$, can be obtained, in concert with other reported values (*9*). Clearly, care must be exercised when determining the time-temperature relationship for glass hydration.

The results obtained in this work also have several important ramifications for the long-term containment of nuclear waste glass.

1) Hydration of nuclear defense waste glass occurs rapidly, even at moderate temperatures (100° to 200°C) similar to those that may be found in repositories, and this hydration radically alters the surface of the glass that might eventually contact ground water. Using the present data and extrapolating the Arrhenius behavior to 90°C for 1000 years, we predict a layer thickness of more than 175 μm as well as encasement of the entire hydrated glass in a matted, claylike mineral.

2) The observed cracking of thick layers suggests that leach tests encompassing humid-dry cycling of hydrated glass may yield results different from the results for fresh glass and may simulate an important repository scenario.

3) The apparent Arrhenius behavior of the glass hydration process suggests that realistic long-term aging of glass may be simulated if one accelerates the reaction process by increasing the temperature. Such tests, if done in combination with other simulated aging reactions, would be valuable in demonstrating whether a waste form can meet projected Nuclear Regulatory Commission requirements.

J. K. BATES
L. J. JARDINE*
M. J. STEINDLER
Chemical Engineering Division,
Argonne National Laboratory,
Argonne, Illinois 60439

References and Notes

1. I. Friedman and R. L. Smith, *Am. Antiq.* **25**, 476 (1960).
2. I. Friedman and W. Long, *Science* **191**, 347 (1976).
3. M. F. Kaplan, *Ancient Materials Data as a Basis for Waste Form Integrity Projections* (Report TR-1749-1, Department of Energy, Washington, D.C., 1980).
4. R. C. Ewing and R. F. Haaker, *Naturally Occurring Glasses: Analogues for Radioactive Waste Forms* (Report PNL-2776, Battelle Pacific Northwest Laboratories, Richland, Wash., 1979).
5. W. A. Lanford, *Science* **196**, 975 (1977).

6. R. R. Lee *et al.*, *Nature (London)* **250**, 44 (1974).
7. D. E. Clark, C. G. Pantano, Jr., L. L. Hench, *Corrosion of Glass* (Books for Industry and the Glass Industry, New York, 1979).
8. I. S. T. Tsong, C. A. Houser, N. A. Yusef, R. F. Messier, W. B. White, J. W. Michels, *Science* **201**, 339 (1978).
9. *Advances in Obsidian Glass Studies*, R. E. Taylor, Ed. (Noyes, Park Ridge, N.J., 1976).
10. J. E. Ericson, in *Scientific Basis for Nuclear Waste Management*, J. G. Moore, Ed. (Plenum, New York, 1981), vol. 3, p. 282.
11. *Fed. Regist.* **48** (No. 130), 35280 (1981).
12. J. E. Mendel *et al.*, *A State-of-the-Art Review of Materials Properties of Nuclear Waste Forms* (Report PNL-3802, Battelle Pacific Northwest Laboratory, Richland, Wash., 1981).
13. J. K. Bates, L. J. Jardine, M. J. Steindler, *The Hydration Process of Nuclear Waste Glass: An Interim Report* (Report ANL-82-11, Argonne National Laboratory, Argonne, Ill., 1982).
14. This work was performed under the auspices of the Department of Energy.

* Present address: Bechtel National, Inc., San Francisco, Calif.

8 February 1982; revised 21 April 1982

Evidence of High Natural Radiation Doses in Certain Mid-Water Oceanic Organisms

Abstract. *Concentrations of the naturally occurring radioactive nuclide polonium-210 were determined in mid-water crustaceans and fish from depths to 1500 meters. Unusually high levels were found in certain categories of organisms, indicating that these organisms were exposed to a particularly high natural radiation dose. The results have implications in terms of possible radiation effects, as a baseline against which artificial radioactive nuclides can be compared, and as a potential technique for studying the feeding behavior of mid-water organisms.*

Radon emanated from the earth's crust decays in the atmosphere and gives rise to a natural radioactive fallout of its descendants ^{210}Pb, ^{210}Bi, and the alpha-particle emitter ^{210}Po (*1*). This fallout is deposited over the oceans as well as the continents, and ^{210}Po is particularly concentrated by most marine organisms (*2*). As a result, the natural radiation dose received by such organisms is usually substantially higher than that received by man. The published data for ^{210}Po in marine organisms were reviewed in 1974 (*2*) and expanded in subsequent publications (*3–8*). Almost all of these data were obtained from animals collected in surface or shallow waters; very limited information has been available concerning material from greater depths in the ocean (*7, 8*).

We report here ^{210}Po concentrations in several crustaceans and fish from depths to 1500 m and in a few deep benthic crustaceans. The extremely high concentrations we found in some cases imply that certain categories of marine animals are exposed to a natural radiation dose which is, to our knowledge, the highest yet reported. These data are of interest for several reasons. (i) The implications of the exposure of a section of the biosphere to a particularly high natural radiation dose over the entire period of biological evolution could be of fundamental importance. (ii) Low-level radioactive waste is already being dumped in the oceans on a small scale, and subseabed disposal in deep ocean sediments has been discussed as a high-level waste disposal option (*9*). The possible hazards arising from the uptake of artificial radioelements into marine organisms will have to be assessed carefully, and such assessment will be difficult because of the lack of data on radiation effects at the low activity levels likely to be encountered. Comparison with the natural radiation dose seems inevitable, and since ^{210}Po provides more than 90 percent of this dose to most marine organisms (*2*) it is important that our knowledge of ^{210}Po concentrations in mid-water and deep-sea organisms be as complete as possible. (iii) The involvement of ^{210}Po in the oceanic biological cycle is extensive, and the nuclide has been shown to be a useful tracer of marine biological processes (*6, 8*). The data reported here support our earlier suggestion (*6, 8*) that ^{210}Po studies can provide useful information about the feeding behavior of certain organisms.

Polonium-210 determinations were made by the standard technique of acid digestion, spontaneous deposition of ^{210}Po from an acid solution onto a silver disk, and counting of the ^{210}Po alpha radioactivity on the disk with ZnS(Ag) scintillation phosphors (*8, 10–12*). The technique is simple, efficient, and highly reproducible; experience with several hundred marine organism samples over a period of many years has shown that our deposition efficiency for ^{210}Po is 98 ± 2 percent. For an individual sample, the major contribution to the error is the statistical counting error. Most of our errors are between 5 and 10 percent. The results of more than 70 measurements on whole animals are reported in Table 1. Almost all the samples were provided by colleagues in other institutions (*13*).

The data in Table 1 are to be compared with published data for ^{210}Po in the same types of organisms from surface and shallow waters. Our data for amphipods, copepods, euphausiids, and mysiids show ^{210}Po concentrations that are generally comparable with those reported for surface samples; the significance of any differences cannot be established until more data are available. A typical value for ^{210}Po in entire fish, mostly from surface waters, has been given as 1.5 pCi/g (*2*); the range of published values, covering more than 50 samples, is from 0.3 to 26 pCi/g (*2*). (All values are given on the basis of dry weight.) Only our Gonostomatidae are at the typical level; the other three families have medians at or beyond the upper end of the range for surface fish. Pentreath *et al.* (*7*) reported that ^{210}Po concentrations in organs and tissues from fish (Alepocephalidae, Gadidae, Macrouridae, and Squalidae) caught between 500 and 1250 m were generally similar to those observed for surface fish. Our data indicate that certain categories of mid-water fish contain consistently high levels of ^{210}Po. On the basis of four species of shrimp caught below 600 m, we suggested (*8*) that mid-water shrimp are significantly higher in ^{210}Po than those from surface waters. Nine more species are represented in the shrimp from 610 to 1500 m in Table 1, and Table 2 shows the ^{210}Po concentration for each of the 13 species from below 600 m. In the mid-water penaeids ^{210}Po ranges from 25 to 117 pCi/g with a median of 43 pCi/g; in eight species of pelagic penaeids from surface waters (*8*) the range was 6.6 to 23.6 pCi/g with a median of 15.7 pCi/g. Of the mid-water penaeids those from the genera *Gennadas* and *Bentheogennema* all have higher ^{210}Po levels than those from the genus *Sergestes*. The same feature is observed in the penaeids from 50 to 760 m (not listed in Table 2): a single *Gennadas* species has a ^{210}Po concentration of 98 pCi/g, while four species of *Sergestes* have 11 to 33 pCi/g. The mid-water carids (9 to 21 pCi/g; median, 14 pCi/g) also have higher ^{210}Po levels than five carid species from surface waters (*8*) (1.3 to 10.4 pCi/g; median, 5.2 pCi/g). The penaeid-carid difference discussed previously (*8*) is again observed; penaeids, which are more primitive in the evolutionary sense, have higher ^{210}Po levels than carids at all three depths (Table 1). The two bathypelagic shrimp samples from 4000 m have ^{210}Po levels typical of surface rather than of mid-water shrimp; more measurements are needed to determine whether this is generally the case.

The following categories of marine organisms from the mid-water region (600 to 1500 m) appear to have consistently high whole-animal ^{210}Po contents: carid